VLA antennas as a function of Elevation

M.Kesteven

VLA Test Memorandum No. 171

ABSTRACT

This note examines the evidence for gravitational distortions of the VLA antennas with changing elevation. There is clear evidence for a lateral shift of the subreflector; a distortion of the main reflector has probably been detected. A number of sub-reflectors could profitably be adjusted to minimise the gain changes over the observing range of elevation.

1. Introduction

A number of independent investigations have produced evidence for antenna changes as a function of elevation:

1. Direct measurement of the subreflector droop (C.Wade).
2. Gain variation with elevation (P.Crane).
3. K-band holography at two different elevations.
4. K-band beam patterns at a range of elevations.

2. Subreflector Droop

In April, 1990 C.Wade and C.Janes carried out theodolite measurements on the subreflector position as a function of elevation. The results are summarised in table 1.

Antenna	#5, in the AAB
Elevation range	90°to 10°
Shift parallel to the elevation axis	< 0.01 inch (< 0.25mm)
Shift in the vertical plane	0.63 inch (16.0mm)

3. Gain Changes

P.Crane examined the gain corrections at 22GHz in VLA Test Memo. # 159 (1989). This data was revised (and reformatted) by J.Wrobel in the VLA Test Memo # 164 (1992). Most antennas have a gain curve which is roughly symmetrical about elevation 45°, with a change of ~ 10% between 45°and the horizon.

We expect a gain change with subreflector offsetof the form:

$$\Delta G = C \cdot \left(\frac{Offset}{\lambda}\right)^2$$

Batilana and Hills (1992) found C = 1.2 for the Cambridge shaped 32m antenna. This suggests a droop (between 45°and the horizon) of about 9mm.

4. K-band Holography

Two K-band holography surveys have been made of the VLA antennas, one at ~ 30°(March 1993), the other at ~ 60°(June 1993).

4.1. Subreflector Offsets

In the analysis of the holography data we explicitly search for the characteristic signature of a subreflector offset. We find excellent agreement between the two surveys, for the offset in the direction parallel to the elevation axis; we find a systematic difference in the vertical plane. The results are summarised in table 2.

Mean Difference in subreflector offset, between the 2 surveys:

parallel to Elevation axis	0.2 ± 0.3
vertical plane	6.2 ± 0.4
axial (focus)	-1.8 ± 0.3

4.2. Reflector Shape

There are 11 antennas common to both surveys. Their surface error maps show excellent agreement between the surveys, so elevation effects, if any, are small. In figure 1 we show the mean difference between the two surveys:

Mean map = <(map at 30°) - (map at 60°)>

where "< .. >" denotes an average over 10 antennas. (Antenna #18 was excluded from the average since its 2cm defect would overwhelm the average).

The contour interval in the image is 0.2mm, starting at ± 0.1mm. The grey scale is based on the magnitude of the error; the sign must be deduced from the contour type (solid if positive).

The mean difference shows a syatematic pattern: raised section on the low side (6 o'clock); lowered sections at 10 and 2 o'clock; and a raised section near the upper subreflector support leg, at its connection with the backup structure.

5. Beam Patterns

In July 1993 a set of beam patterns were obtained at regular intervals, following a radio source (W49N) from transit to the horizon. The scans were in pairs, azimuth, then elevation. Some examples of the patterns are shown in figure 2. The principal results are:

1. The leading elevation sidelobe (on the high side of the antenna) decreases by 8 ± 1 dB between 65°and 10°.
2. The trailing elevation sidelobe increases by 6 ± 1 dB.
3. Both azimuth sidelobes increase by 2 ± 0.5 dB.
4. An encouraging proportion of the antennas are optimised (in the sense of equal sidelobes) in the elevation range 40°to 50°.

The results are illustrated in figure 3. Each row in figure 3 relates to a single antenna; the left hand panel shows the normalised antenna gain relative to the normalised gain of antenna #14 at the same elevation; the next two panels relate to the subreflector offset. For each scan we take the ratio to the sidelobes adjacent to the main beam; this ratio (in dBs) is proportional to the subreflector offset. At present the scale factor is not well determined. (The ratio is less sensitive to calibration, compression and blockage problems. The magnitude of the coma lobe would otherwise be preferred).

In table 3 we list the subreflector adjustments required to bring the subreflector on axis at 45°. The convention adopted to define the displacement directions is: looking into an antenna which is pointing at the horizon, N is up, E is to the right, S is down and W to the left.

antenna	Azimuth displacement (mm)	Elevation displacement (mm)
1	5 E	17 N
2	2 E	20 N
3		
4	2 W	2 N
5	1 E	0
6	2 W	0
7	7 W	1 S
8	5 W	1 N
9	?	9 S
10	5 W	5 S
11	2 W	5 N
12	3 W	0
13	1 W	12 N
14	7 W	0
15	3 E	0
16		
17	5 E	1 N
18	5 W	10 N
19	1 E	1 N
20	1 E	2 N
21	0	8 N
22	8 W	0
23		
24	8 W	1 S
25	6 W	5 S
26	0	8 N
27	7 W	17 S
28	10 W	7 N

The offsets here are in fair agreement with the subreflector offsets computed in the holography surveys, with the notable exception of antennas 1 and 2. It should also be noted that the holography values refer to the "conic-section" approximation used in the analysis, and so are $\sim 30\%$ too large.

6. Discussion

In figure 4 we compare the elevation at which the elevation sidelobes are equal to the elevation at which the gain is maximised. The correlation is excellent, which suggests that the subreflector offset is the prime determinant of the gain/elevation dependance.

The magnitude of the subreflector shift ($\sim 16mm$) should be reflected in the antenna pointing model: we could expect the "sag" term to be ~ 7 arcminutes. But this is not observed: the average sag term is 0.3 arcminutes. One explanation would be that the reflector itself deforms with elevation, with a rotation of the optical axis and a shift of the vertex.

Antenna #21 is distinctly anomalous: it shows little elevation dependance.

7. Conclusions

There is now a good deal of evidence of a changing offset between the reflector axis and the subreflector axis with changing elevation. The consequences can be minimised by ensuring that the subreflector is on axis at a mid-range elevation .. say 45°. About twelve antennas should be optimised. A further twelve should be repositioned in the direction parallel to the elevation axis. Table 3 contains the settings.

VLA. Gravitational distortion signature?

June: ~ 60° EL for the central regions (uv plane)

March: ~ 30° EL   May in March – June

Plot file version 4 created 29-JUN-1993 15:42:48

MAR-JUN.DIFF.9

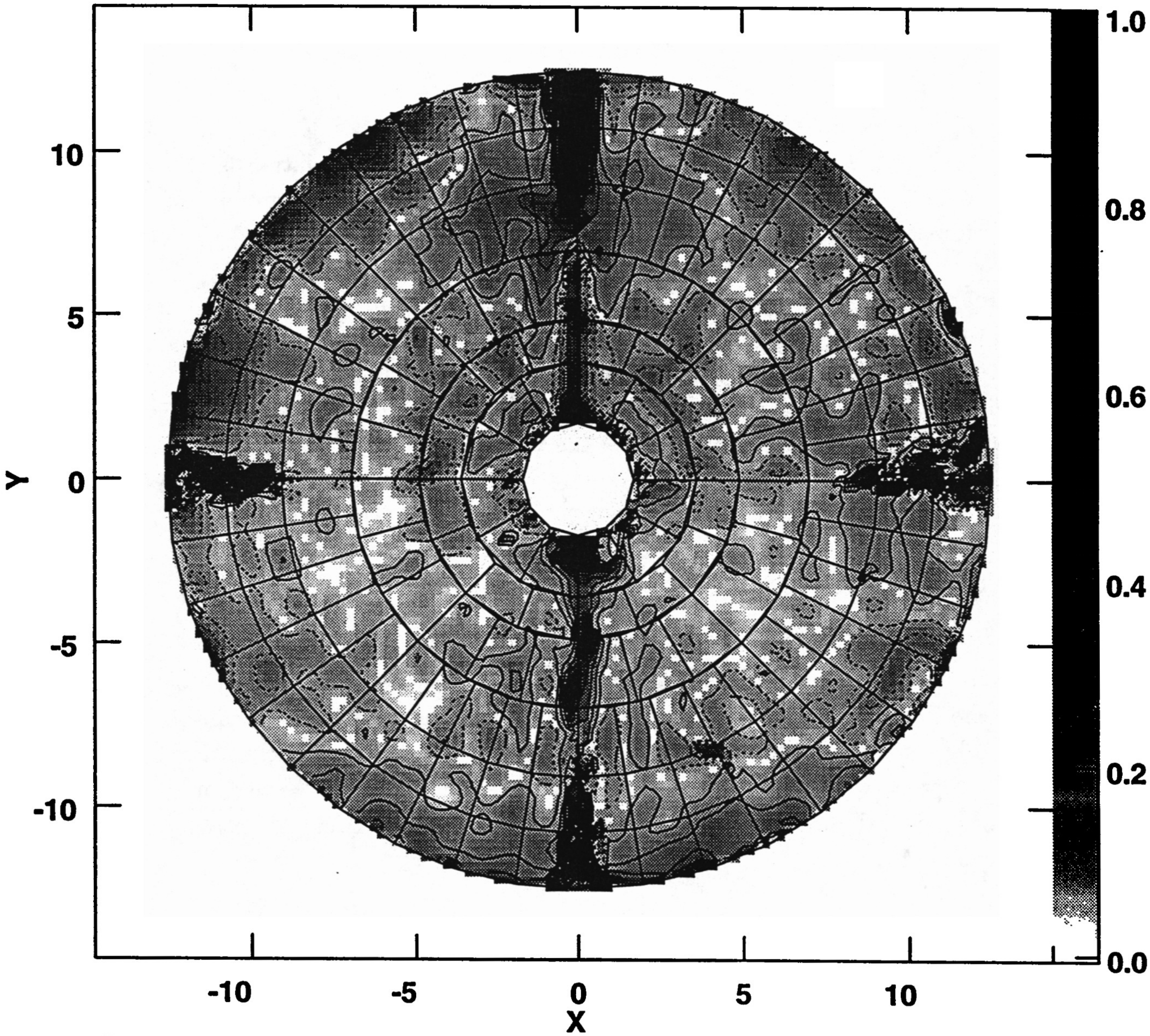

Grey scale flux range= 0.000 1.000 MilliMeter
Peak contour flux = 5.3916E-03 Meter
Levs = 1.0000E-04 * (-9.00, -7.00, -5.00, -3.00, -1.00, 1.000, 3.000, 5.000, 7.000, 9.000)

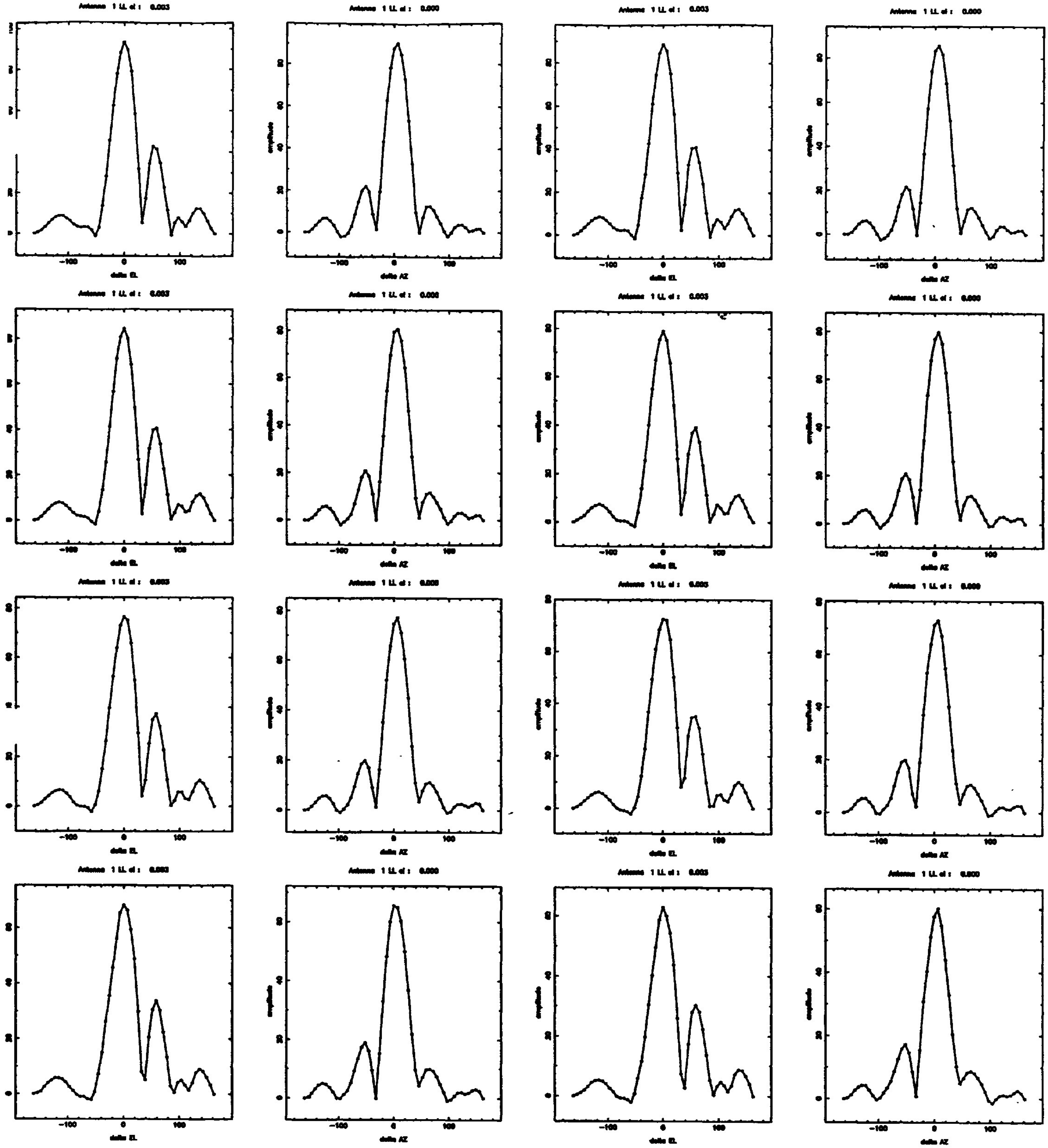

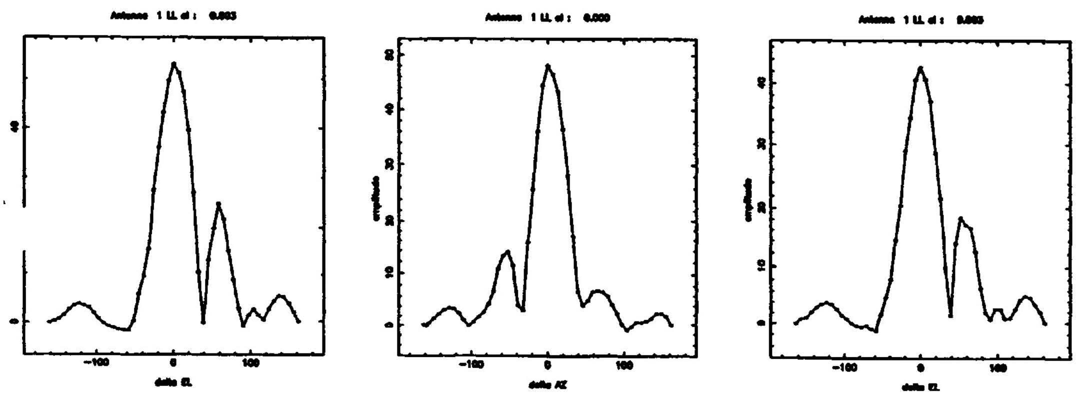

Antenna 1.
Voltage Beam patterns

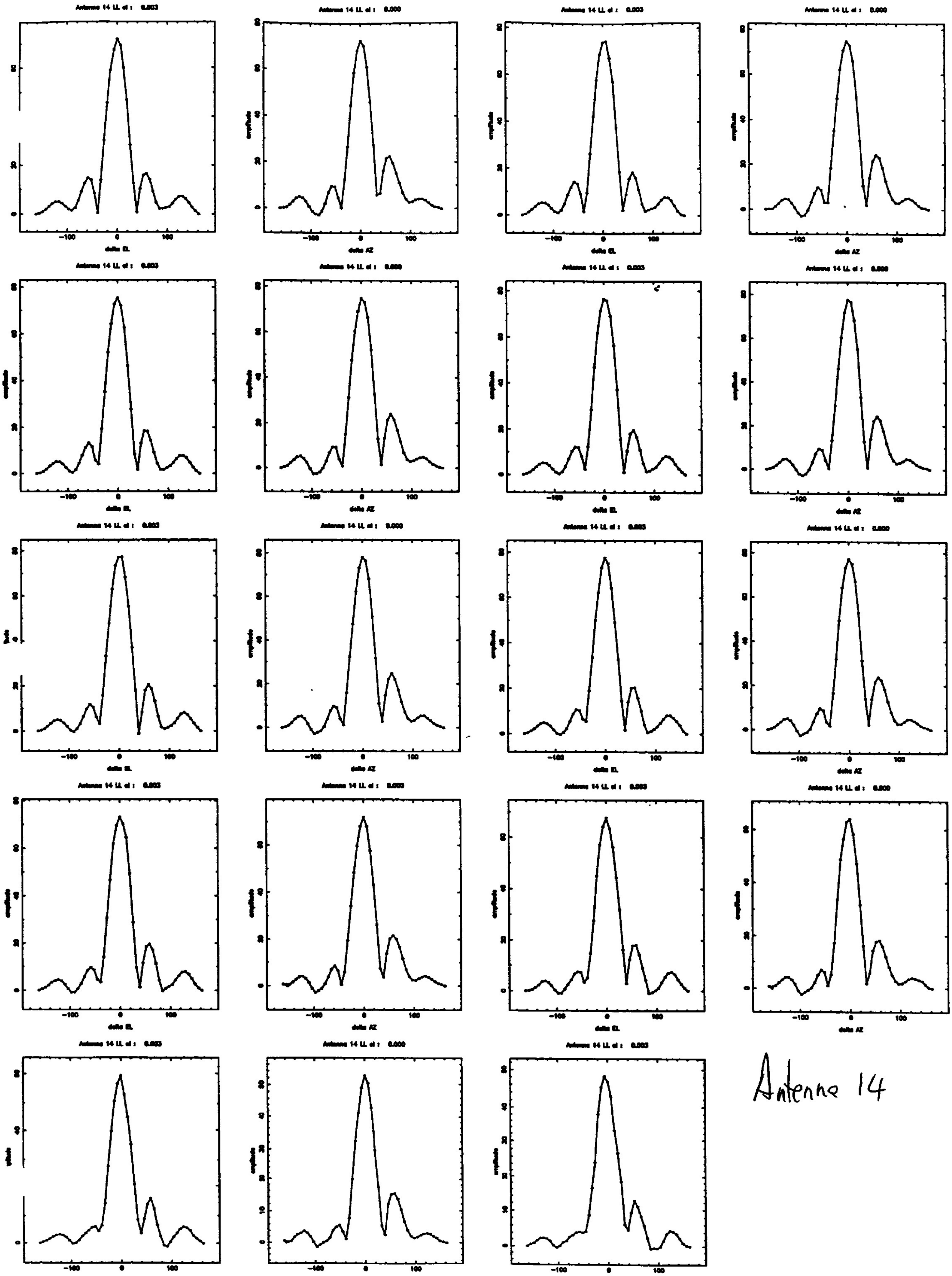
Antenne 14 LL el : 0.003
Antenne 14 LL el : 0.000
amplitude
delta EL
delta AZ
-100
0
100

Antenne 14

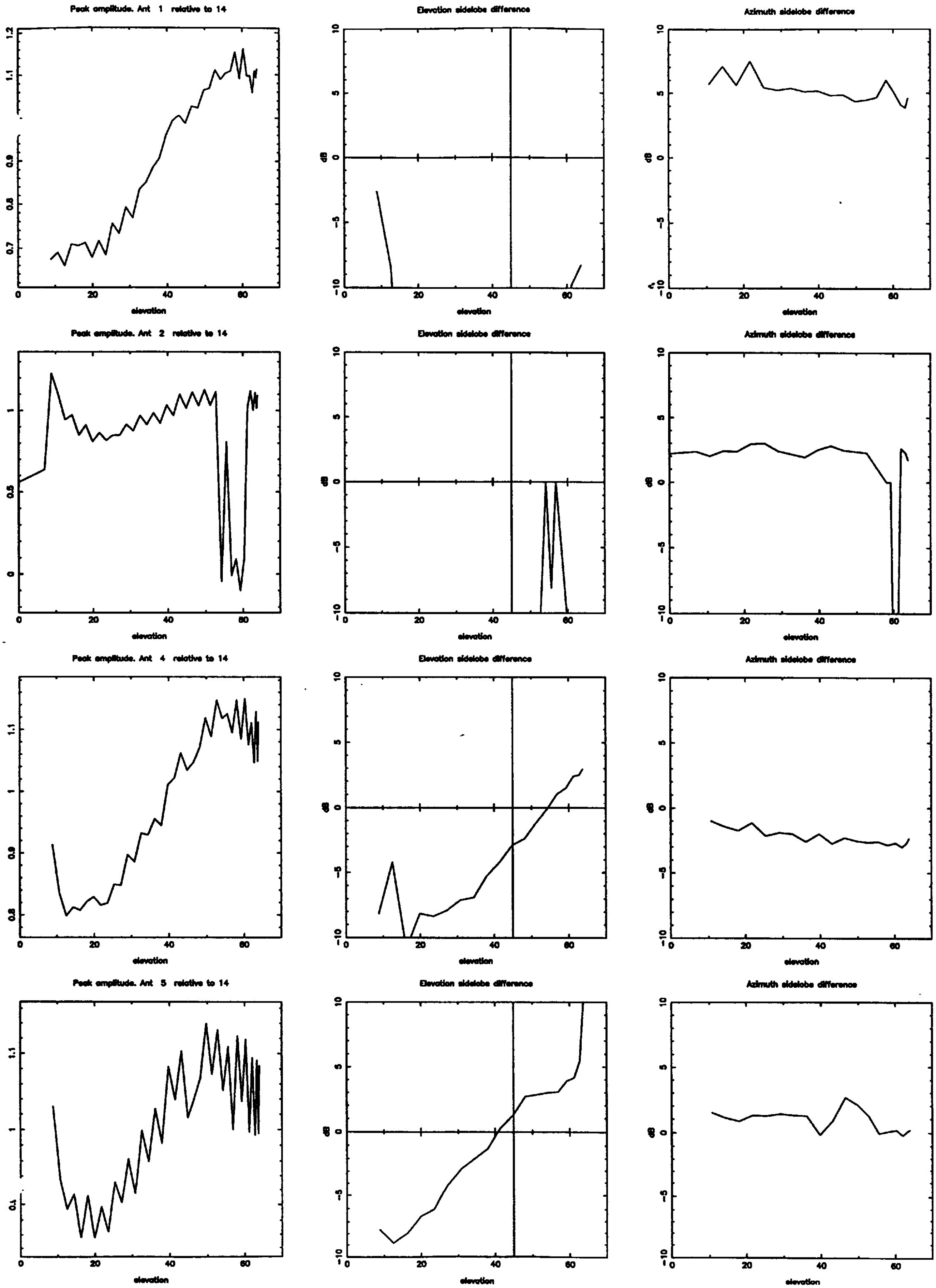

Peak amplitude. Ant 1 relative to 14
Elevation sidelobe difference
Azimuth sidelobe difference
Peak amplitude. Ant 2 relative to 14
Elevation sidelobe difference
Azimuth sidelobe difference
Peak amplitude. Ant 4 relative to 14
Elevation sidelobe difference
Azimuth sidelobe difference
Peak amplitude. Ant 5 relative to 14
Elevation sidelobe difference
Azimuth sidelobe difference
elevation
dB

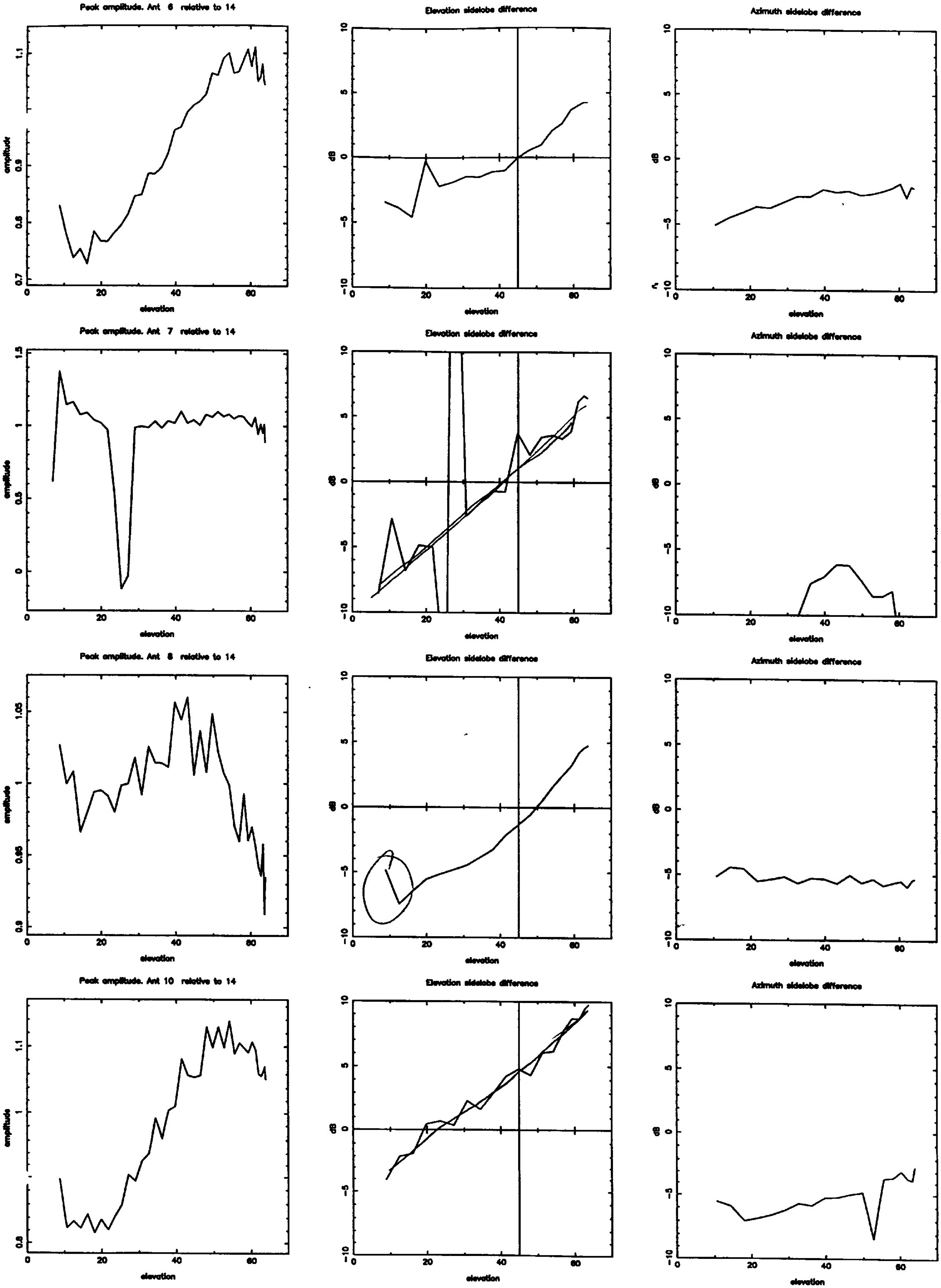

Peak amplitude. Ant 6 relative to 14
Elevation sidelobe difference
Azimuth sidelobe difference
Peak amplitude. Ant 7 relative to 14
Elevation sidelobe difference
Azimuth sidelobe difference
Peak amplitude. Ant 8 relative to 14
Elevation sidelobe difference
Azimuth sidelobe difference
Peak amplitude. Ant 10 relative to 14
Elevation sidelobe difference
Azimuth sidelobe difference
amplitude
dB
elevation

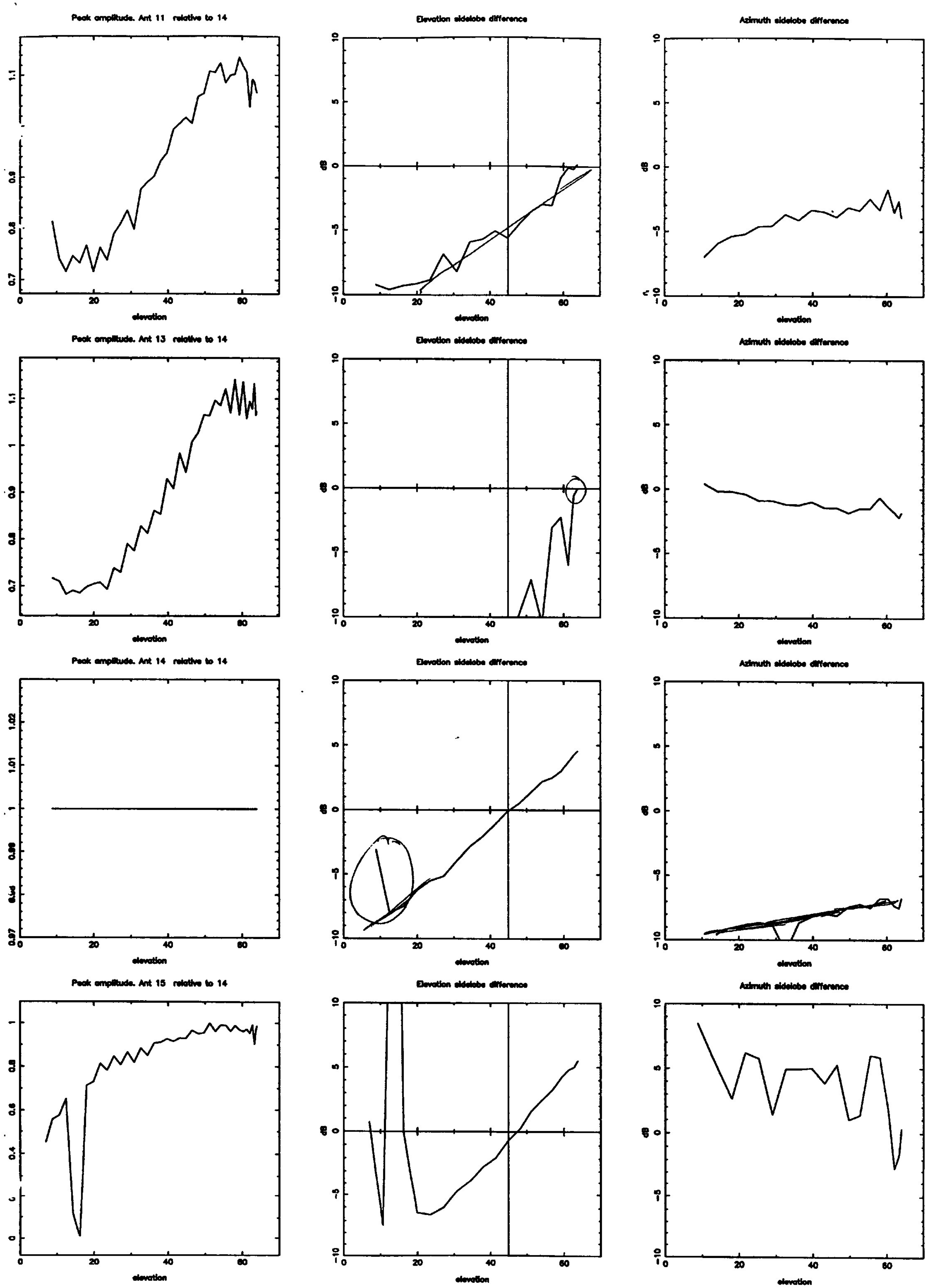
Peak amplitude. Ant 11 relative to 14
Elevation sidelobe difference
Azimuth sidelobe difference
Peak amplitude. Ant 13 relative to 14
Elevation sidelobe difference
Azimuth sidelobe difference
Peak amplitude. Ant 14 relative to 14
Elevation sidelobe difference
Azimuth sidelobe difference
Peak amplitude. Ant 15 relative to 14
Elevation sidelobe difference
Azimuth sidelobe difference
elevation
dB

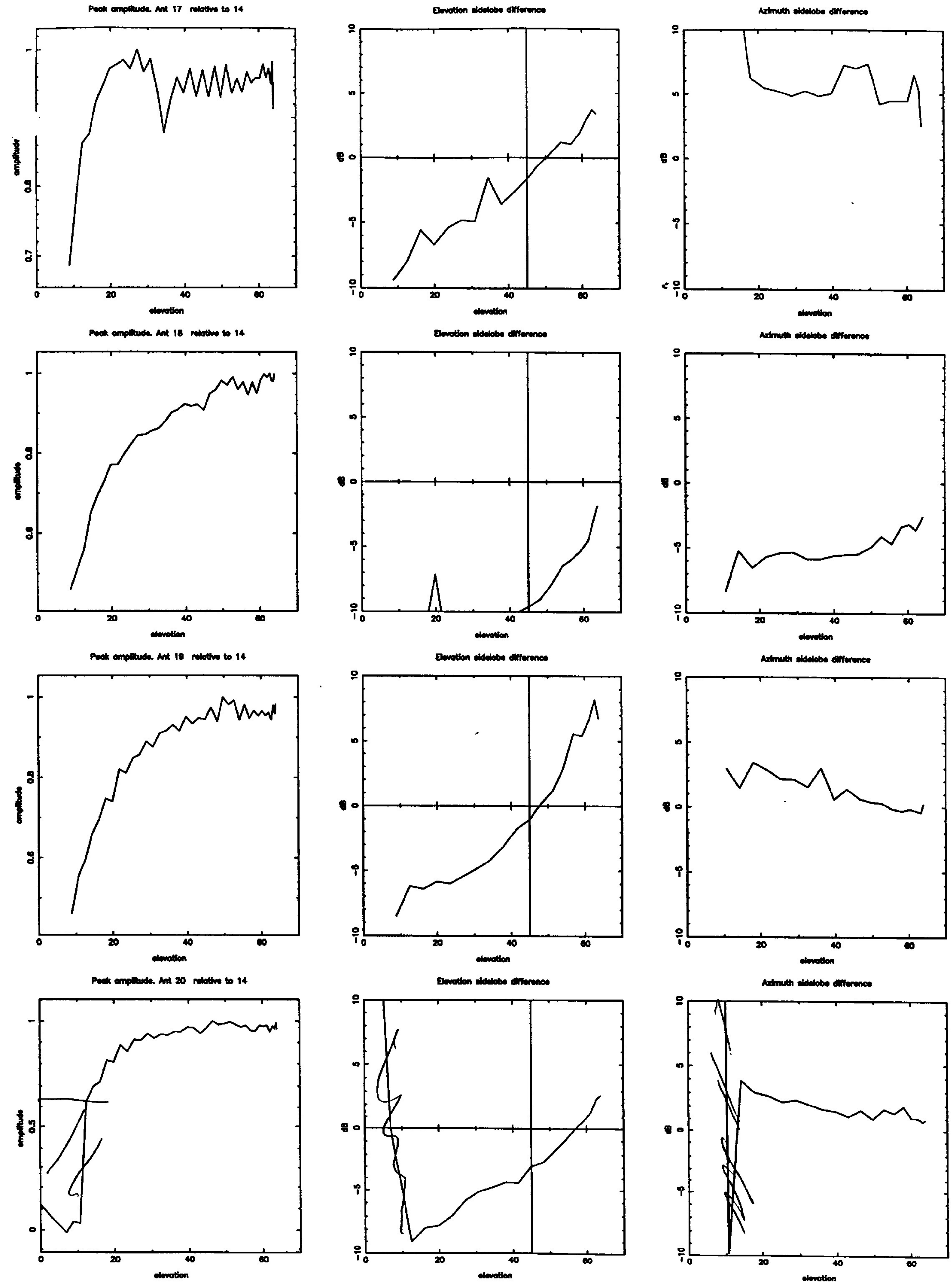

Peak amplitude. Ant 17 relative to 14
Elevation sidelobe difference
Azimuth sidelobe difference
Peak amplitude. Ant 18 relative to 14
Elevation sidelobe difference
Azimuth sidelobe difference
Peak amplitude. Ant 19 relative to 14
Elevation sidelobe difference
Azimuth sidelobe difference
Peak amplitude. Ant 20 relative to 14
Elevation sidelobe difference
Azimuth sidelobe difference
amplitude
dB
elevation

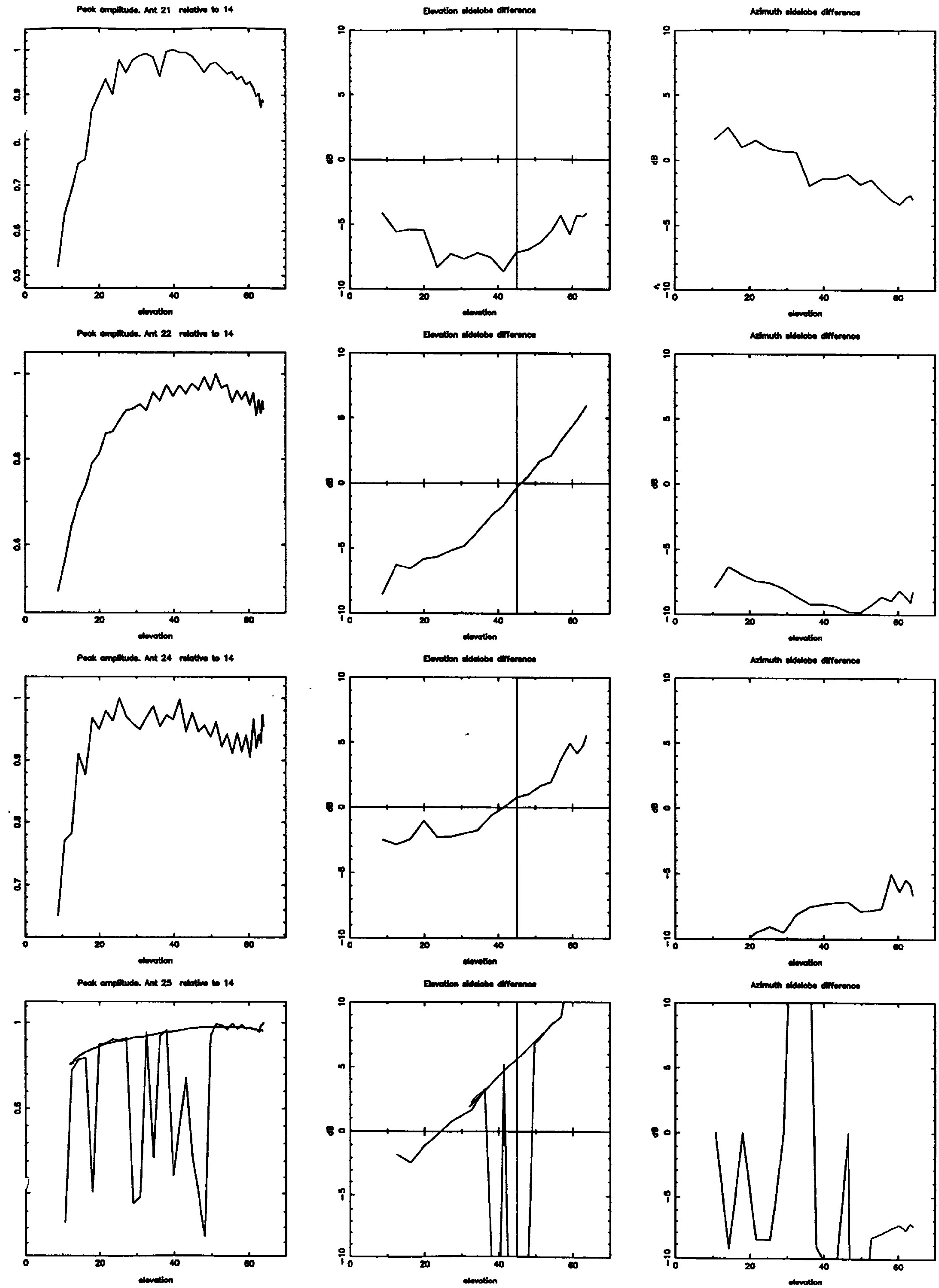
Peak amplitude. Ant 21 relative to 14
Elevation sidelobe difference
Azimuth sidelobe difference
Peak amplitude. Ant 22 relative to 14
Elevation sidelobe difference
Azimuth sidelobe difference
Peak amplitude. Ant 24 relative to 14
Elevation sidelobe difference
Azimuth sidelobe difference
Peak amplitude. Ant 25 relative to 14
Elevation sidelobe difference
Azimuth sidelobe difference
elevation
dB

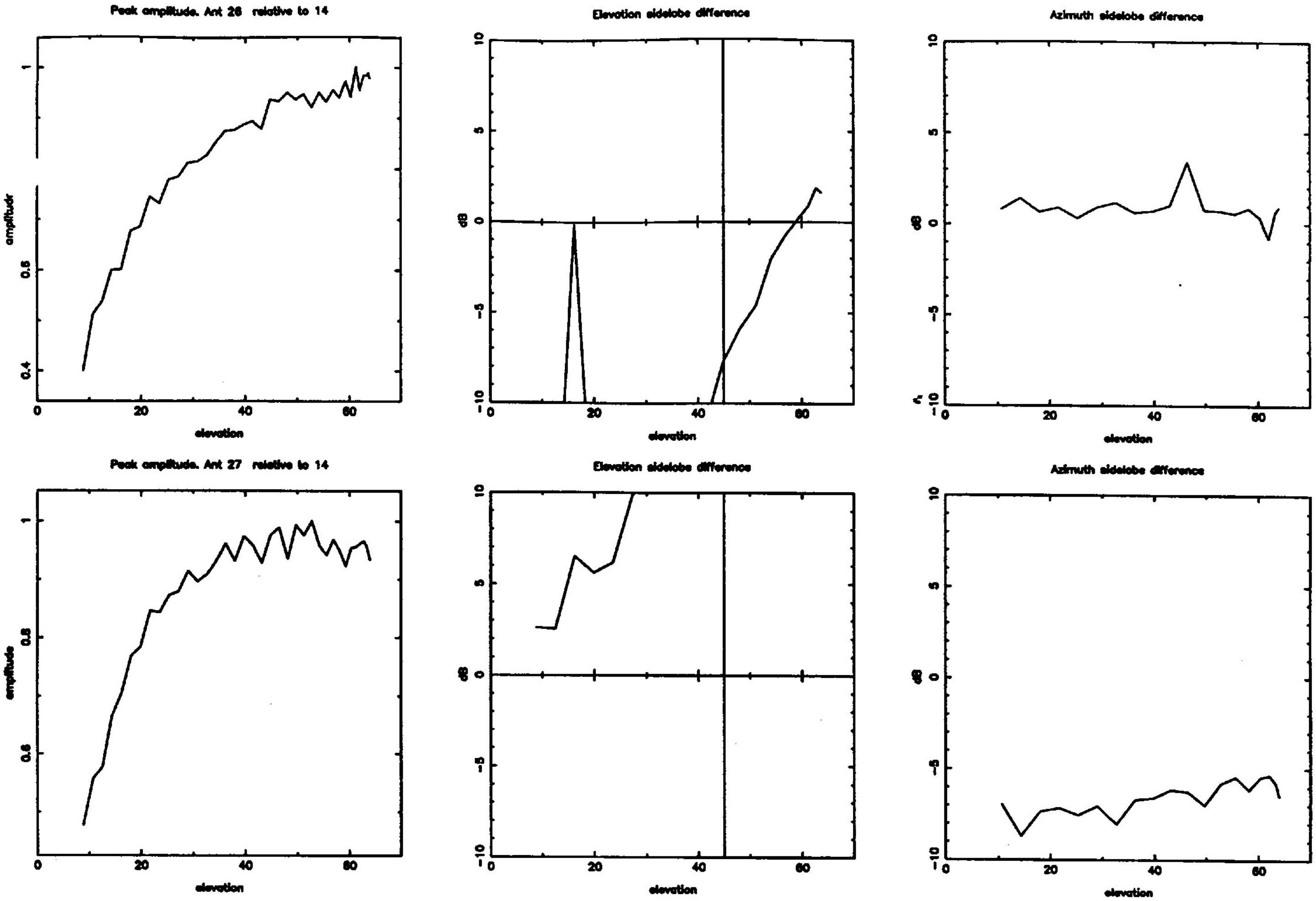

Peak amplitude. Ant 26 relative to 14
amplitude
elevation
Elevation sidelobe difference
dB
elevation
Azimuth sidelobe difference
dB
elevation
Peak amplitude. Ant 27 relative to 14
amplitude
elevation
Elevation sidelobe difference
dB
elevation
Azimuth sidelobe difference
dB
elevation

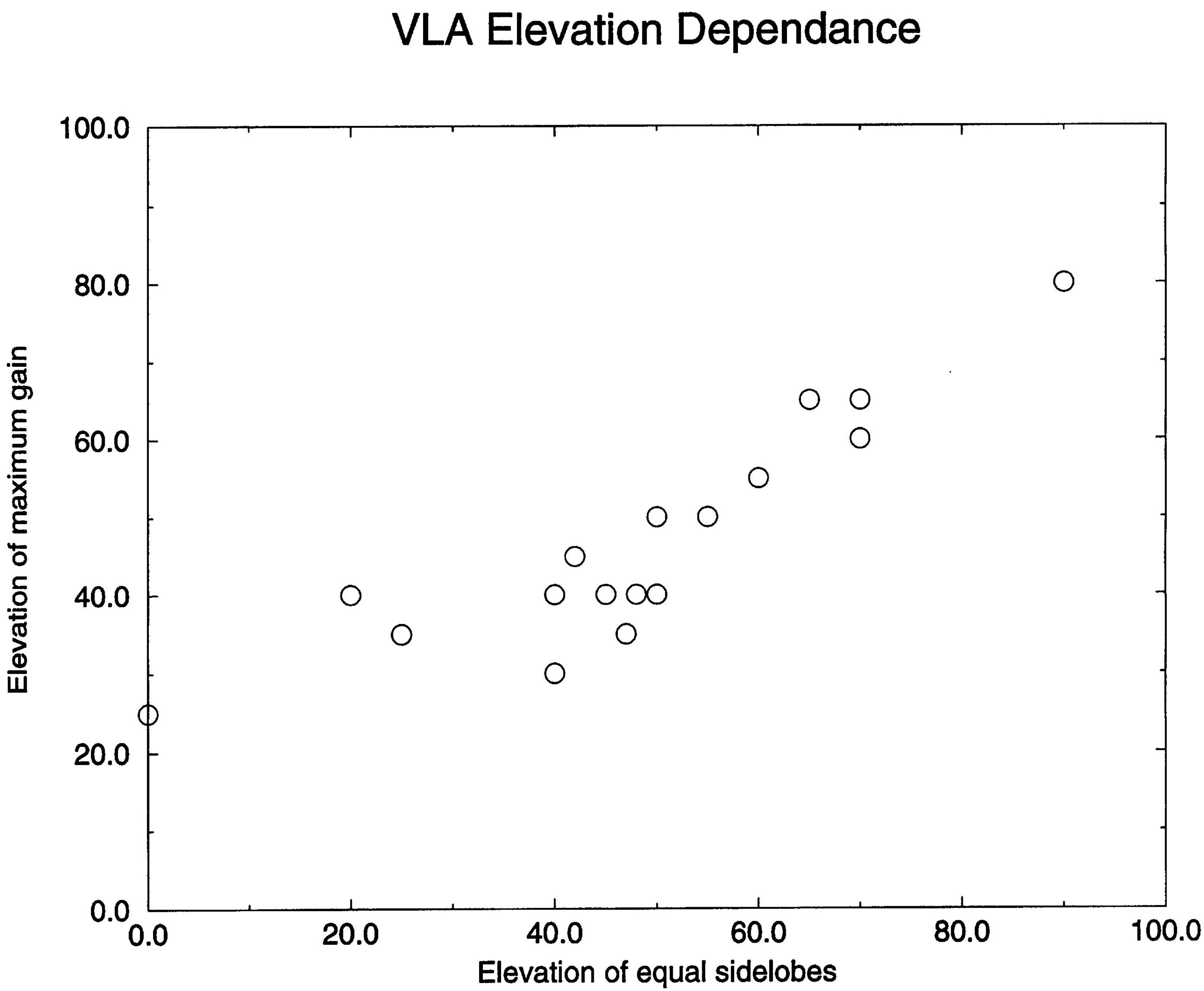

VLA Elevation Dependance
100.0
80.0
60.0
40.0
20.0
0.0
Elevation of maximum gain
0.0
20.0
40.0
60.0
80.0
100.0
Elevation of equal sidelobes